Desalination and Water Treatment
www.deswater.com
doi: 10.1080/19443994.2014.980330

57 (2016) 2052–2063
January

Taylor & Francis
Taylor & Francis Group

Investigation of Cu(II) removal by cobalt-doped iron oxide captured in PVA-alginate beads

Ee Ting Wong, Kian Hwa Chan, Muhammad Irfan, Ani Idris*

Faculty of Chemical Engineering, Department of Bioprocess Engineering, c/o Institute of Bioproduct Development, Universiti Teknologi Malaysia, 81310 UTM Johor Bahru, Johor, Malaysia, Tel. +60 7 553 5603; Fax: +60 7 558 8166; email: ani@cheme.utm.my (A. Idris)

Received 11 April 2014; Accepted 16 October 2014

ABSTRACT

Polyethylene glycol-coated magnetic nanoparticles of Co-Fe_2O_3 were prepared by a simple co-precipitation method and embedded in polyvinyl alcohol (PVA)-alginate beads to remove the Cu(II) from the aqueous solution. The performance of Cu(II) removal was then investigated by adding the PVA-alginate Co-Fe_2O_3 beads into the Cu(II) synthetic solution at various operating condition. The results showed that the removal of Cu(II) by the synthesized beads was pH dependent and the optimal pH for Cu(II) removal was at pH 6 with 8% nanoparticle loading. The Cu(II) adsorption onto the adsorbent could also be characterized well using Langmuir and Freundlich isotherm with $R^2 > 0.95$.

Keywords: Cu(II) removal; PVA-alginate beads; Adsorption isotherm; Recyclability

1. Introduction

Copper is one of the important trace elements required by human's body for enzyme synthesis, tissues and bones development [1]. However, the divalent copper (Cu^{2+}) is toxic and carcinogenic and the elevated intake of Cu^{2+} sometimes may cause death, particularly in children [2]. Therefore, the rapid and effective removal of copper from water stream is very important in order to maintain the Cu^{2+} permissible limit of 1.5 mg/L (World Health Organization Standard) in drinking water so as to protect the environment and public health [3]. The conventional method to remove the Cu(II) from the water stream includes chemical precipitation process [4], membrane filtration method [5], electrochemical treatment [6], and adsorption [7]. Among all, adsorption is simple, highly effective, and the most cost-effective method [8–11].

In heavy metal-contaminated wastewater treatment, iron oxide is used widely due to its non-toxicity, biocompatibility, biodegradability, low particle dimension, large surface area, and suitable magnetic properties [12]. In order to facilitate the separation of nanoparticle from water after the adsorption process as well as to improve the recyclability of the adsorbent, we embedded the synthesized nanoparticle in the stable matrix of polyvinyl alcohol (PVA)-alginate. This matrix enables the nanoparticle to disperse uniformly throughout bead structure and improve the adsorption of the Cu(II) ions [13], and the overall representation for the preparation of our adsorbent is shown in Fig. 1.

In this research, cobalt was used to modify the iron oxide since the substitution of iron (Fe^{2+}) in an iron oxide with other transition metals or metal ions such

*Corresponding author.

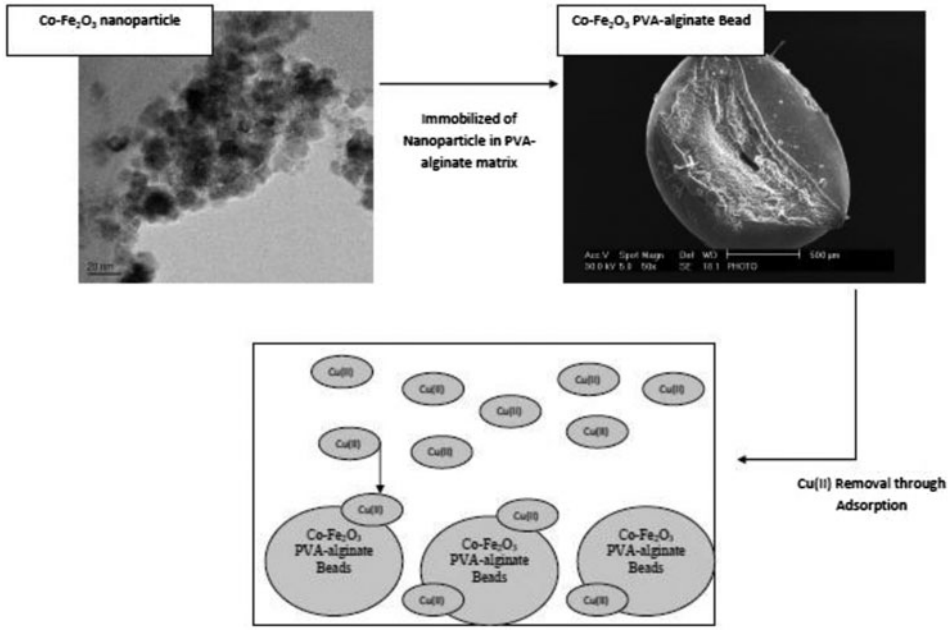

Fig. 1. Immobilized of Co-Fe_2O_3 nanoparticle in the PVA-alginate matrix to form the beads to removal Cu(II) from the aqueous solution.

as nickel, cobalt, and aluminum was reported to improve the performance of the iron oxide [14–16]. So in this study, the Co was used as the dopant to form the nanoparticles which had better performance than the native iron oxide nanoparticles.

In this research, the effective parameters on the batch removal such as initial pH and nanoparticle loading were investigated, the Cu(II) adsorption kinetics were also evaluated by Langmuir isotherm, Freundlich isotherm, and Lagergren kinetic model [17]. Finally, the adsorbents were examined its sorption recovery through adsorption–desorption experiment to further investigate its potential usage in the heavy metal wastewater treatment.

2. Methodology

2.1. Materials

Cobalt chloride and ferric chloride salts were purchased from QREC Chemical. Sodium hydroxide, hydrogen peroxide, sodium sulfite, and polyethylene glycol (PEG MW-600) were also supplied by Merck. Nitric acid (HNO_3, 65%, v/v), hydrochloric acid (HCI, 37%,v/v), acetone, and PVA 184000 were supplied from Aldrich Chemicals whereas sodium alginate, boric acid, and calcium chloride were provided by Fluka Chemie GMGH. The chemicals used for preparing standard metal solution were copper (II) sulfate salt from Sigma Aldrich and distilled water.

2.2. Synthesis of doped Co-Fe_2O_3 nanoparticles coated with PEG

In this study, the cobalt-doped iron oxide was synthesized through co-precipitation method. PEG was used as the nanoparticle-coated surfactant since it is the cheapest, non-toxic, and soluble in both polar and some non-polar solvents; thus, it is quite inert to chemical treatments and biocompatible [18–20].

Nanoparticles of Co-Fe_2O_3 were synthesized using high purity salts of $CoCl_2{\cdot}6H_2O$ (99%) and $FeCl_3{\cdot}9H_2O$ (98%). The salts were mixed in 1:2 ratios and homogenized. The mixture was stirred for several minutes, and sodium hydroxide solution (0.6 M) was added drop by drop. The magnetic ($CoFe_2O_4$) precipitate was formed once the sodium hydroxide was added. Then, the particles were collected and washed several times with distilled water to remove unwanted residual of salt. Nitric acid was used to acidify the precipitate obtained so that a reversion of the surface charges can be provoked and the precipitate was further oxidized into Co-Fe_2O_3 at 90˚C [21]. The magnetic wet slurry was then dispersed in PEG MW-600 at the temperature of 80˚C for 1.5 h, and distilled water was then added as the carrier.

2.3. Characterization of Co-Fe_2O_3 nanoparticles before PVA-alginate matrix entrapment

Fourier transform infrared (FT-IR) (PerkinElmer IR Spectroscopy v 5.3) was used to confirm that the PEG

coating was successful while the mean Co-Fe_2O_3 nanoparticles size was characterized by transmission electron microscope (TEM) (JEM-2010F) and composition of the nanoparticles was determined by X-ray diffraction (XRD).

2.4. PVA-alginate magnetic beads preparation

A mixed solution of PVA and sodium alginate and a mixed solution of boric acid and $CaCl_2$ were used to synthesize the PVA-alginate magnetic beads using the method reported by Zain et al. [13]. Alginate was used to improve the surface properties of the beads by preventing the agglomeration. Hundred milliliters of precursor solution was prepared by mixing 12 g of PVA, 1 g of alginate, and 8 mL of PEG-coated Co-Fe_2O_3 in distilled water, and the precursor solution was dropped and stabilized in boric acid and calcium chloride solution to obtain the spherical beads with 8% nanoparticle loading.

2.5. Cu(II) removal evaluations

The synthesized PEG-coated Co-Fe_2O_3 nanoparticle immobilized PVA-alginate separable beads was then tested for its Cu(II) removal under several parameters such as pH and nanoparticle loading. Fifty milliliters of 100 mg/L of synthetic Cu(II) solution was placed in a batch reactor and then treated with 5.0 g of Co-Fe_2O_3 PVA-alginate beads for 3 h. The pH of the solution was adjusted using NaOH or HCI. The concentration of Cu (II) in the solution was determined by the modified method which was described by Aksu [22] and then determined at 460 nm using the UV-spectrophotometer (Shimadzu UVmini-1240). To investigate the optimum nanoparticle loading for Cu(II) removal, the beads was synthesized by the methods reported above by varying the nanoparticle percentage (% v/v) in the PVA-alginate beads, respectively.

The Cu(II) removal efficiency of the adsorption beads (8% nanoparticle loading; pH 6 ± 0.5) was also tested with the coexist of inorganic chemical oxidant and reductant since the presence of oxidant and reductant was reported to effect the performance of the adsorbent for heavy metal removal [23,24]. Hydrogen peroxide and sodium sulfite were chosen as our coexist compounds in this study since both of these compounds were used widely in disinfection and dechlorination process particularly in the domestic water purification plant [25,26]. The concentrations of the additives were varied from 0.5 to 7% to study their coexist effect on the adsorbent performance.

2.6. Adsorption kinetics

The kinetic studies of adsorption of Cu(II) using PEG-coated Co-Fe_2O_3 PVA-alginate adsorbent were performed by fitting the experimental data obtained into the Langmuir adsorption isotherm and Freundlich isotherm model. Lagergren 1st and 2nd order adsorption dynamic kinetic were then used to fit the adsorption kinetic data.

2.7. Adsorption–desorption experiment

Consecutive adsorption–desorption cycles were used to examine the reusability of the beads. The adsorption experiment was conducted by setting the 5.0 g of adsorbent into the separate beakers contained 50 mL of 50 mg/L of Cu(II) synthetic solution at pH 6. After 3 h of treatment, the adsorbent from each beaker was stirred moderately with desorbing agent (HCl 50 mL of 0.1 M) in 250-mL Erlenmeyer flasks for 60 min at room temperature and the concentration of Cu(II) desorbed was then measured. The regenerated beads were recycled and used again for another four repeated sorption–desorption cycles so as to investigate on their regenerate behavior [27].

3. Results and discussion

3.1. Characterization of Co-Fe_2O_3 nanoparticles and Co-Fe_2O_3 PVA-alginate beads

Fig. 2(a) shows the TEM images of PEG-coated Co-Fe_2O_3 nanoparticles which were synthesized and undergone the crystal lattice formation at 90°C using the co-precipitation method. Under the TEM image, most of the nanoparticles are found to be spherical in shape. The distributions of nanoparticles are able to fit into the Gaussian curve with mean size of 11.736 ± 3.499 nm. Fig. 2(b) shows the XRD of the PEG-coated Co-Fe_2O_3 nanoparticles. The nanoparticle exhibits a slight shift of main peak (311) at 35.50° (JCPDS 39–1346) to 35.5° due to the introduction of Co onto the Fe_2O_3 nanoparticles [28,29].

Fig. 3 shows the FT-IR spectrum of PEG-coated-Co-Fe_2O_3 nanoparticles (Fig. 3(b)) as well as the nanoparticle immobilized PVA-alginate beads (Fig. 3(a)). The –OH bond stretching at 3,500–3,200 cm^{-1} indicates the presence of PEG, which was successfully coated on the Co-Fe_2O_3 crystal lattice (Fig. 3(b)). The coated PEG would act as the surfactant, which prevents the agglomeration of nanoparticle and improves the dispersion of nanoparticle in its carrier therefore would ease the dispersion of nanoparticle throughout the nanoparticle matrix [12]. The nanoparticle immobilized

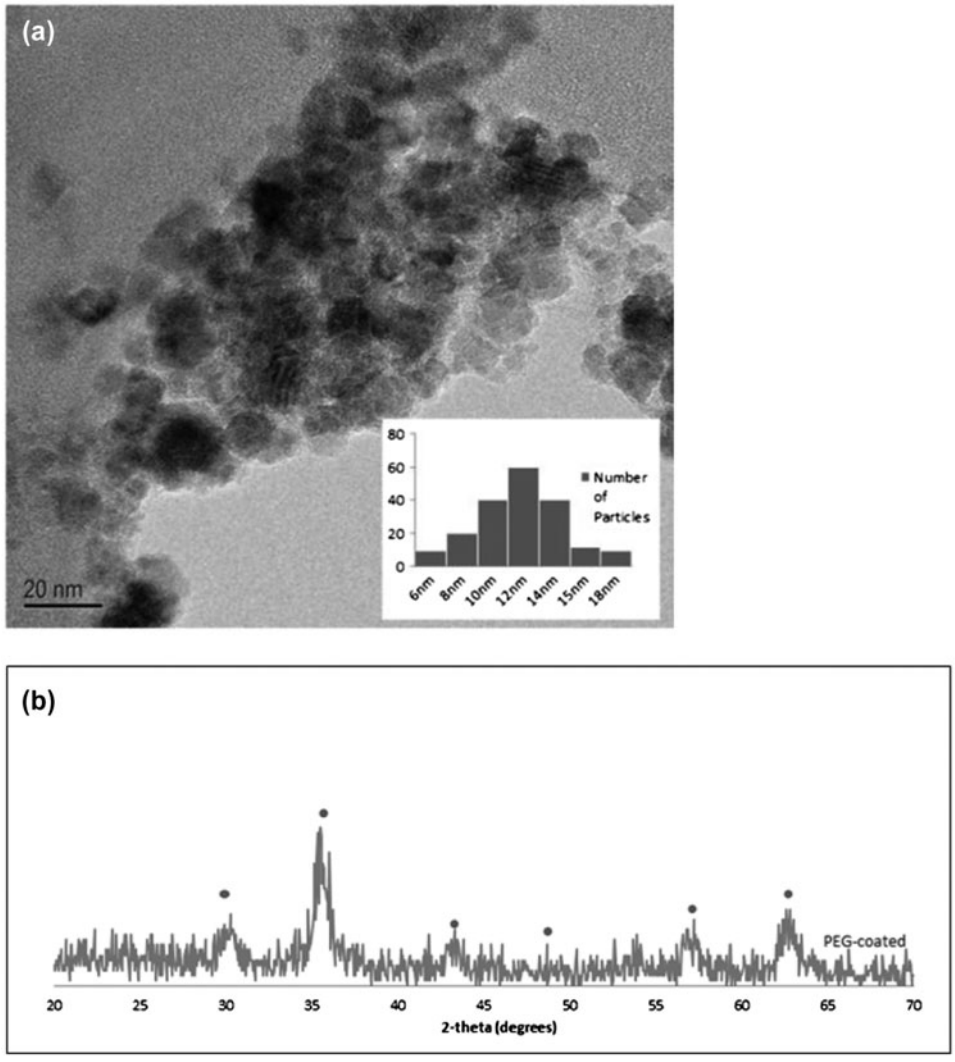

Fig. 2. (a) TEM images of PEG coated Co-Fe_2O3 Nanoparticles; (b) XRD of PEG-coated Co-Fe_2O3 Nanoparticles.

PVA-alginate beads also exhibit broader –OH stretching due to the higher composition of –OH groups contributed by the PVA-alginate matrix (Fig. 3(a)).

Fig. 4 shows the scanning electron microscope (SEM) image of the Co-Fe_2O_3 PVA-alginate beads. The beads exhibit pore internal structure and therefore increase the surface area for the Cu(II) adsorption. These porous structures also enable the diffusion of Cu(II) into the beads easily.

3.2. *Effect of pH on Cu(II) removal and stability of the Co-Fe_2O_3 PVA-alginate beads*

Fig. 5 shows the influence of pH on the Cu (II) removal by Co-Fe_2O_3 PVA-alginate beads. The optimum pH for Cu (II) removal was found to be at pH 6. At the pH solutions lower than 5, hydrogen ions may compete for the adsorption sites on the surface of the Co-Fe_2O_3 PVA beads and this result to a very low adsorption of copper cations. The adsorption of Cu(II) is facilitated when the pH of the solutions increases due to the absent of the H^+ that lowers the electrostatic attraction for Cu(II). However, increasing the pH above 6 is not recommended since it will result to the precipitation of insoluble copper hydroxide, causing a decrease in the adsorption of Cu(II) ions [12].

Energy dispersive X-ray spectroscopy (EDX) was used to analyze the chemical composition on the bead's cross-sectional (Fig. 6(a) and external surface Fig. 6(b)). It found out that the Cu(II) was trapped mainly in the bead internal layer rather than the external surface area since higher concentration of Cu(II)

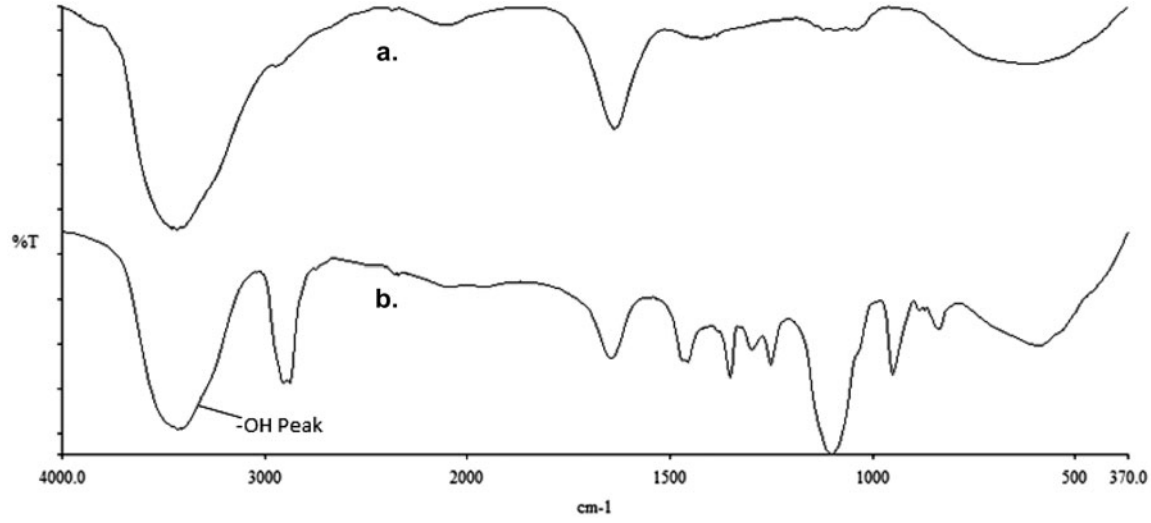

Fig. 3. FT-IR Spectrum of: (a) PEG-coated-Co-Fe_2O_3 PVA-alginate beads; (b) PEG-coated-Co-Fe_2O_3.

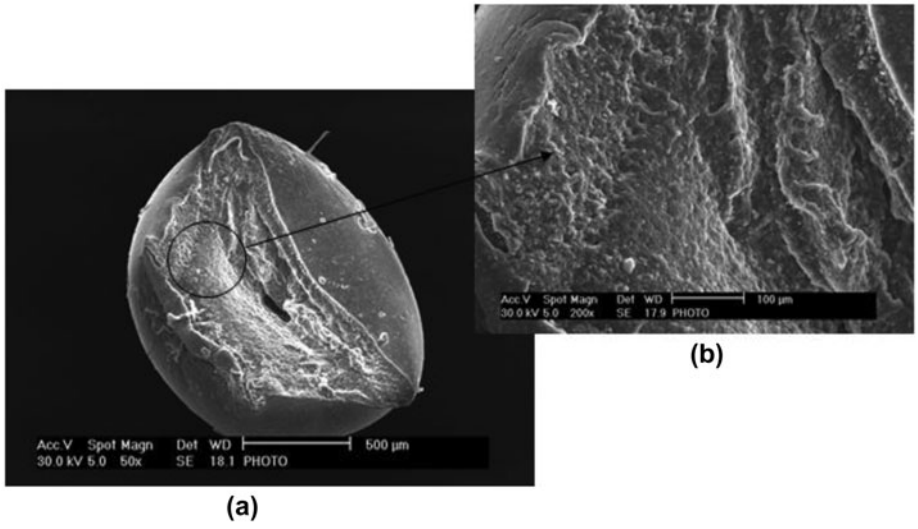

Fig. 4. SEM image of PEG-coated-Co-Fe_2O_3 PVA-alginate beads: (a) cross-section at 50×; (b) cross-section at 200×.

was detected in the cross sectional of the bead. FT-IR spectrum in Fig. 7 shows that the PVA-alginate beads provide a mechanical and chemical stable structure during the Cu(II) removal process since there are no sign of destruction of chemical bonds during the treatment process in pH 6.

3.3. Effect of nanoparticle loading

The results in Fig. 8 revealed that an increase in nanoparticle dosage resulted to an increase in Cu(II) uptake by the Co-Fe_2O_3-PVA-alginate beads. However, further increase of nanoparticle loading above 8% shows only slight improvement in Cu(II) removal percentage because the number of active sites on the adsorbent has exceeded the required amount and probably due to the intervention of mass transfer limitations [27].

3.4. Effect of coexist compounds

H_2O_2 is a popular oxidant widely used in industrial wastewater treatment to remove dyes or organic compounds [30,31]. Fig. 9 shows the effect of H_2O_2 percentage on the Cu(II) removal and beads structure. The addition of H_2O_2 greatly reduces the Cu(II)

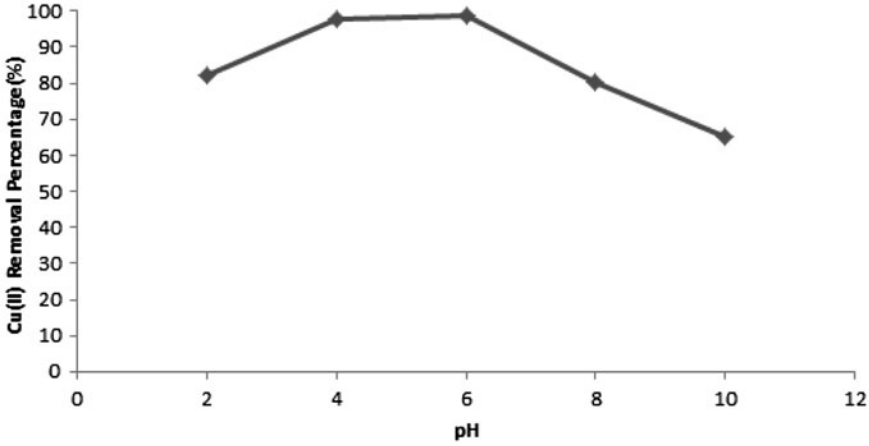

Fig. 5. Effect of pH on Cu(II) removal efficiency.

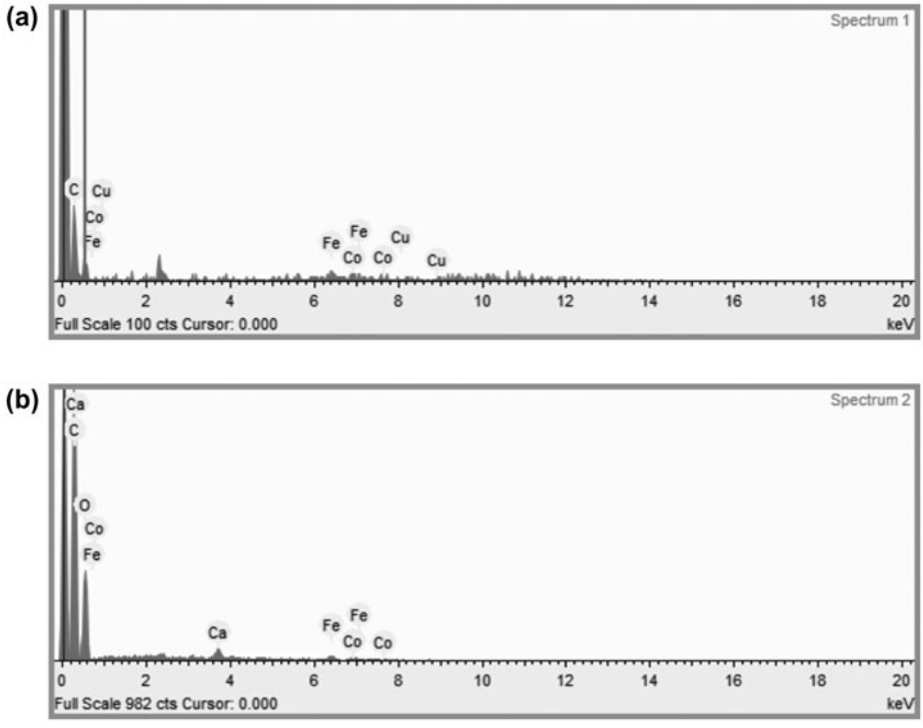

Fig. 6. EDX spectrum shows the chemical composition of: (a) cross-sectional; (b) external surface of the bead after Cu(II) removal treatment.

removal efficiency of the beads which due to the following reasons: Increased H_2O_2 concentration swells the beads due to the rapid formation and accumulation of O_2 inside the beads. The rapid accumulation of H_2O_2 inside the bead ruptures and destroys the PVA–alginate matrix. Degradation of H_2O_2 also produces OH radical which destroys the chemical bonding of the PVA-alginate matrix as shown in the FT-IR spectrum of Fig. 10(c). Besides, the accumulation of oxygen inside the bead renders the diffusivity of Cu(II) through the porous PVA-alginate beads.

While in the presence of sodium sulfite as coexist compounds, it seen to improve slightly the Cu(II) removal performance of the beads as shown in Fig. 11. This may due to the reason that sulfite is highly negative and readily reduced and transfer its electron to

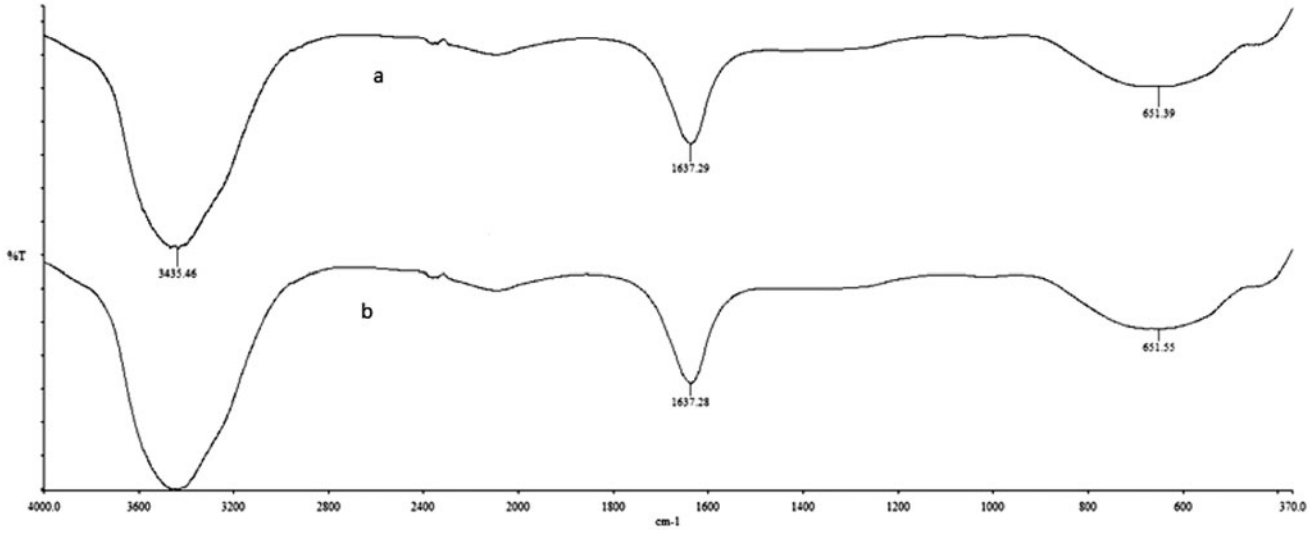

Fig. 7. FT-IR Spectrum of: (a) PEG-coated-Co-Fe_2O_3 PVA-alginate beads before treatment; (b) PEG-coated-Co-Fe_2O_3 PVA-alginate beads after Cu(II) removal treatment.

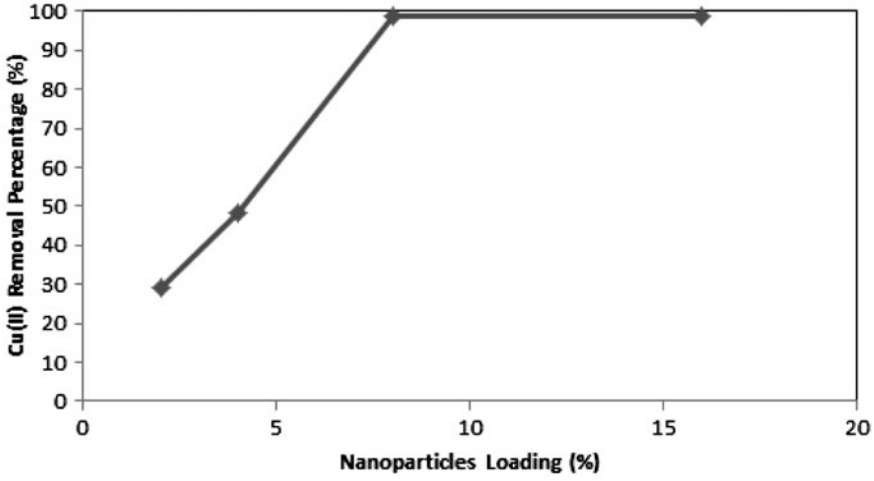

Fig. 8. Effect of nanoparticle loading on Cu(II) removal efficiency.

the adsorbent and will help to stabilize the negative adsorption site of the beads [32], and therefore enable more Cu(II) to be adsorbed.

3.5. Adsorption kinetic

3.5.1. Langmuir isotherm

Langmuir equation is written in the following form:

$$q_e = q_{\max}\frac{K_L C}{1 + K_L C} \quad (1)$$

where q_e and $q_{\max}$ are the adsorption capacity at equilibrium and at maximum, respectively (mg/g), K_L is Langmuir adsorption constant (L/mg) and C is the concentration of the Cu(II) ions in aqueous phase (mg/L). To obtain the K_L and $q_{\max}$, the Langmuir equation is usually linearized in the following form [33–36]:

$$\frac{1}{q_e} = \frac{1}{K_L q_{\max}}\frac{1}{C} + \frac{1}{q_{\max}} \quad (2)$$

The plot of the above linearized equation for adsorption of Cu(II) by $CoFe_2O_3$ PVA-alginate beads is

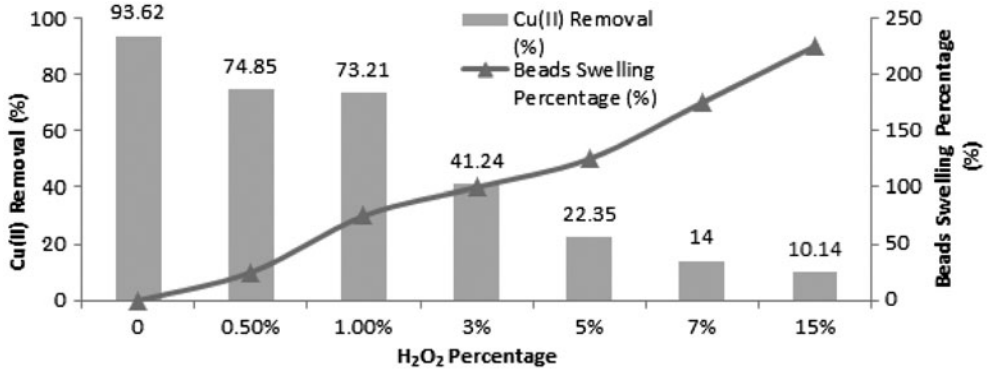

Fig. 9. Effect of H_2O_2 percentage on the Cu(II) removal and the beads swelling percentage.

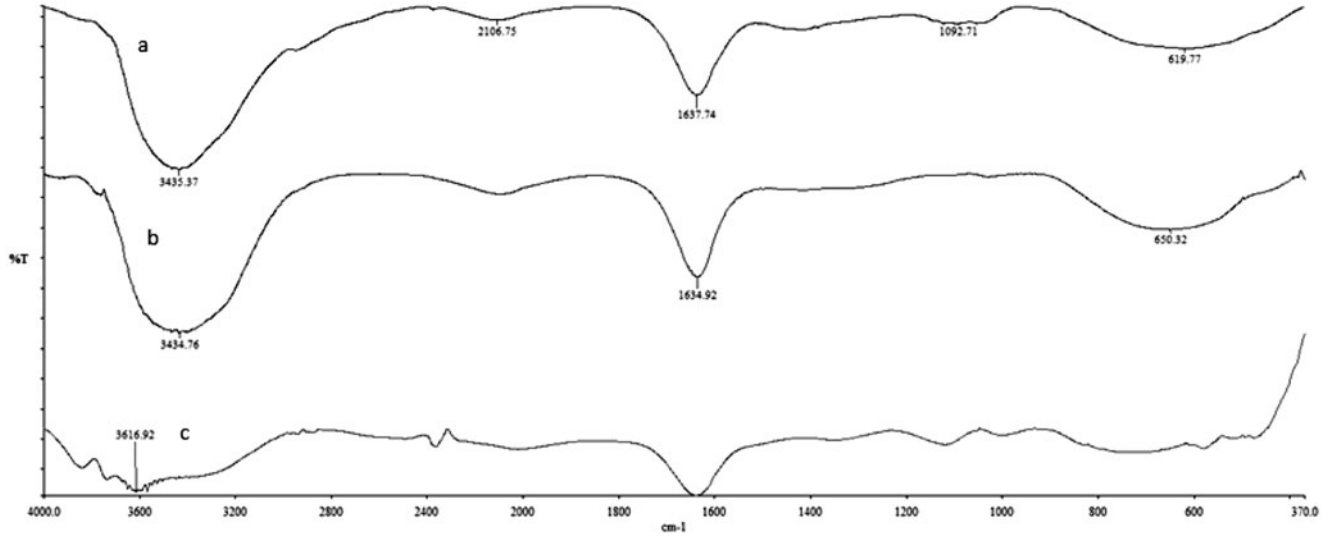

Fig. 10. FT-IR spectrum of the beads under the effect of H_2O_2 oxidant: (a) 0%; (b) 3%; (c) 15%.

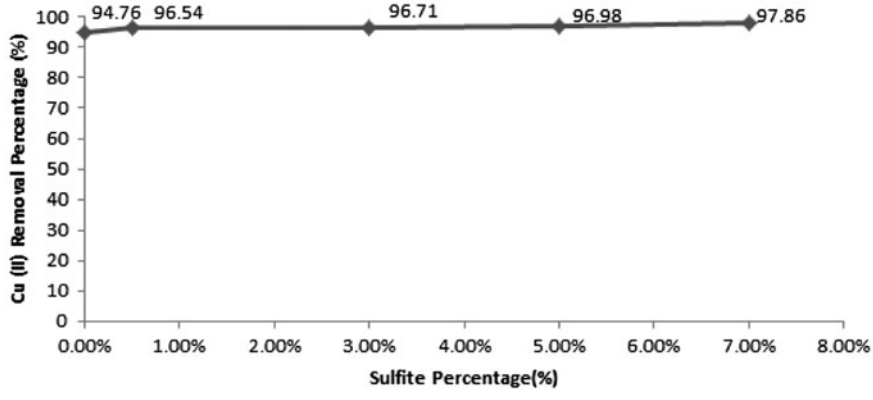

Fig. 11. Effect of sulfite on Cu(II) removal.

shown in Fig. 12(a) and the adsorption parameters are summarized and represented in Table 1 and has the q_{max} of 1.15 mg/g.

3.5.2. Freundlich isotherm

Freundlich isotherm is an empirical equation for the description of adsorption equilibrium. The equation is written as below:

$$q_e = K_F C^{\frac{1}{n}} \tag{3}$$

which can be linearized as following:

$$\log q_e = \log K_F + \frac{1}{n}\log C \tag{4}$$

where q_e is the adsorption capacity at equilibrium (mg/g), K_F and n are Freundlich adsorption constant, which determined empirically [35,36]. The plot of the Freundlich linearized equation for adsorption of Cu(II) PEG-coated $CoFe_2O_3$ PVA-alginate beads is shown in Fig. 12(b), and the adsorption parameters are summarized and represented in Table 1. A favorable adsorption tends to have Freundlich constant n between 1 and 5 whereas the larger value of n (smaller value of $1/n$) implies that stronger interaction between adsorbent and Cu(II) and the adsorption process is favorable [37]. The adsorption of Cu(II) onto the PEG-coated Co-Fe_2O_3 PVA-alginate beads can be fitted into both Langmuir and Freundlich Isotherm with $R^2 > 0.95$. The calculated Freundlich constant $n = 2.471$ which indicated that the Cu(II) adsorption is favorable using this novel adsorbent.

3.5.3. Lagergren kinetic model

One of the significant characteristic to define the performance of adsorption is dynamic adsorption in terms of solute uptake rate, which governs the residence time [38,39]. In order to evaluate the experiment data obtained in the adsorption process, Lagergren pseudo first order and second order are applied.

Lagergren pseudo-first-order equation for Cu(II) removal is generally expressed by the following equation [38,39]:

$$\log (q_e - q_t) = \log (q_e) - \frac{k_1}{2.303} t \tag{5}$$

where q_e and q_t are adsorption capacity at equilibrium and at time t, respectively (mg/g), k_1 is the rate constant of pseudo-first-order adsorption (min^{-1}).

And the pseudo-second-order adsorption kinetic rate equation is presented as:

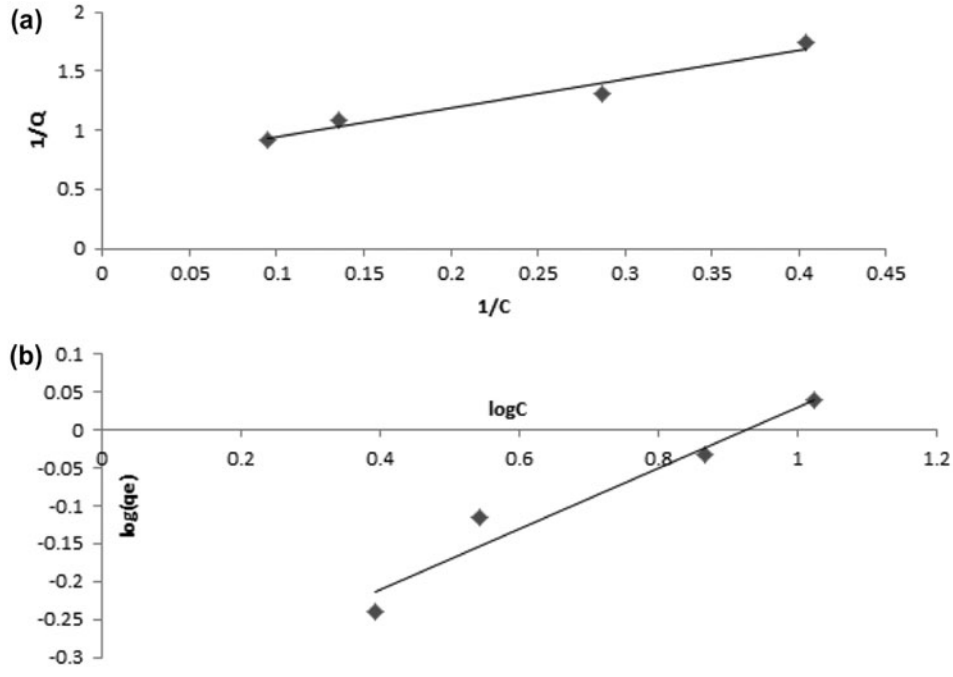

Fig. 12. (a) Plot of linearized equation of Langmuir isotherm; (b) plot of linearized equation of Freundlich isotherm.

Table 1
Adsorption parameters for Langmuir and Freundlich isotherm

Type of adsorbent	Operation condition	Langmuir parameter			Freundlich parameter		
		K_L (L/mg)	q_{max} (mg/g)	R^2	K_F (mg/g)	n	R^2
PEG-coated $CoFe_2O_3$ PVA-alginate bead	27°C, pH 6, nanoparticles loading 8%	0.2793	1.4489	0.9642	0.4233	2.471	0.9494

$$\frac{t}{q_t} = \frac{1}{k_2 q_e^2} + \frac{1}{q_e}(t) \quad (6)$$

where k_2 is the rate constant of the pseudo-second-order adsorption (g mg^{-1} min^{-1}).

Fig. 13 shows the plot of Lagergren first-order and second-order kinetic model with the Cu(II) initial concentration of 40 mg/L. From the plot of the Lagergren kinetic model, we noticed that the removal of Cu(II) by our adsorbents fits more well into the Lagergren second-order kinetic with the correlation coefficient, R^2 of 0.9875 compared to the Lagergren first-order kinetic with the R^2 of only 0.9253. Therefore, the adsorption of Cu(II) ions by the adsorbents is considered as chemisorption mechanism since it could be represented with the second-order kinetic model [40,41].

3.6. Adsorption–desorption experiment

Sorption recovery of the synthesized beads is an important factor since it indirectly determines the costs that associated with the adsorption system. As shown in Fig. 14 for the first cycle, the Cu(II) desorption from the metal ions loaded beads lead to 98.15% metal ions recovery. As shown in Fig. 14(a) and (b), the adsorption and desorption capability for the Cu(II) ions do not reduce considerably during five cycles of

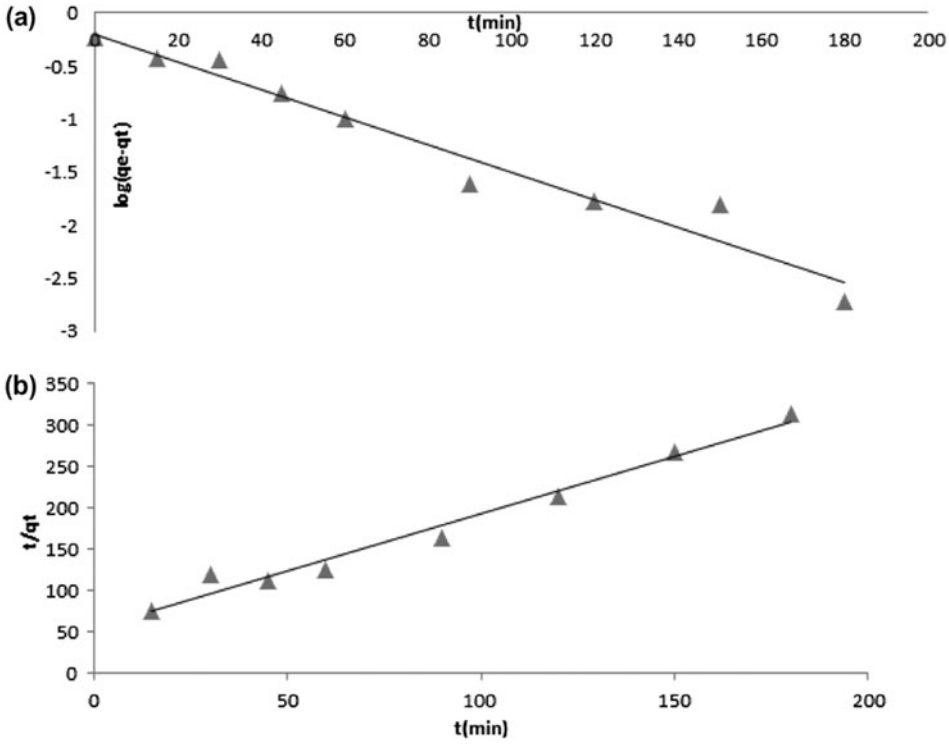

Fig. 13. (a) Plot of Lagergren first-order kinetic model; (b) plot of Lagergren second-order kinetic model.

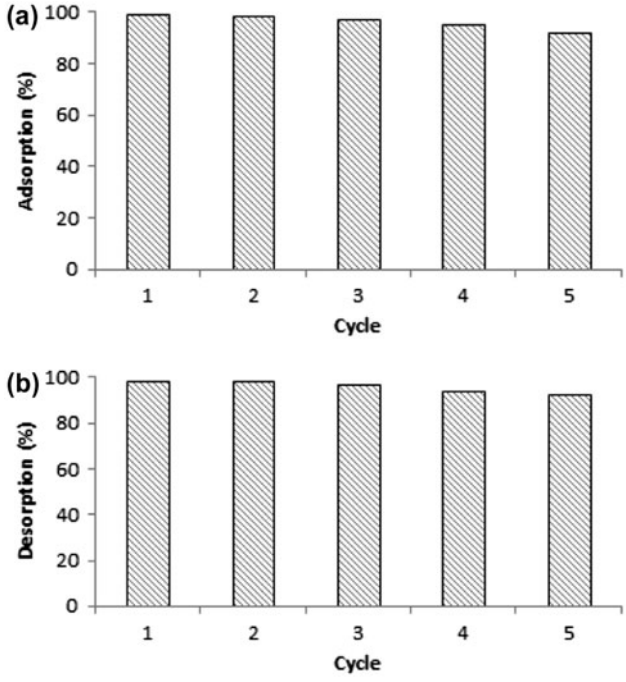

Fig. 14. (a) Adsorption capability of the beads for five cycles; (b) desorption capability of the beads for five cycles.

adsorption–desorption procedure. The beads only experienced a 7% slight reduction in its adsorption capability after five cycles. As a result, the beads can be recycled for more than five times without notably losing their adsorbent properties.

4. Conclusion

The Cu(II) removal rate was greatly affected by the pH and nanoparticles loading during the adsorption process. The result shows that the Co-Fe_2O_3 PVA-alginate beads perform optimally at pH 6 and 8% nanoparticles loading. The Cu(II) adsorption onto the adsorbent could be characterized well using Langmuir, Freundlich isotherm, and Lagergren second-order kinetic model with good R^2. Additionally, the results obtained from the recycled beads indicate that the beads can be reused for at least five times without losing its performance.

Acknowledgment

Financial support from Universiti Teknologi Malaysia (Research University Grant/4F236) for this research is gratefully acknowledged.

References

[1] S.T. Akar, T. Akar, Z. Kaynak, B. Anilan, A. Cabuk, Ã.Z. Tabak, T.A. Demir, T. Gedikbey, Removal of copper(II) ions from synthetic solution and realwastewater by the combined action of dried Trametes versicolor cells and montmorillonite, Hydrometallurgy, 97 (2009) 98–104.
[2] C. Tizaoui, S.D. Rachmawati, N. Hilal, The removal of copper in water using manganese activated saturated and unsaturated sand filters, Chem. Eng. J. 209 (2012) 334–344.
[3] M.N. Mužek, S. Svilović, J. Zelić, Fly ash-based geopolymeric adsorbent for copper ion removal from wastewater, Desalin. Water Treat. 52 (2014) 2519–2526.
[4] M.M. Matlock, B.S. Howerton, D.A. Atwood, Chemical precipitation of heavy metals from acid mine drainage, Water Res. 36 (2002) 4757–4764.
[5] H. Bessbousse, T. Rhlalou, J.F. Verchère, L. Lebrun, Removal of heavy metal ions from aqueous solutions by filtration with a novel complexing membrane containing poly(ethyleneimine) in a poly(vinyl alcohol) matrix, J. Membr. Sci. 307 (2008) 249–259.
[6] I. Heidmann, W. Calmano, Removal of Zn(II), Cu(II), Ni(II), Ag(I) and Cr(VI) present in aqueous solutions by aluminium electrocoagulation, J. Hazard. Mater. 152 (2008) 934–941.
[7] A.A. Bsoul, L. Zeatoun, A. Abdelhay, M. Chiha, Adsorption of copper ions from water by different types of natural seed materials, Desalin. Water Treat. 52 (2014) 5876–5882, doi: 10.1080/19443994.2013.808593.
[8] H. Znad, Z. Frangerskides, Chicken drumstick bones as an efficient biosorbent for copper (II) removal from aqueous solution, Desalin. Water Treat. 52 (2014) 1560–1570, doi: 10.1080/19443994.2013.786657.
[9] Z. Liu, Y. Liu, L. Chen, H. Zhang, Performance study of heavy metal ion adsorption onto microwave-activated banana peel, Desalin. Water Treat. (in press), doi: 10.1080/19443994.2013.841108.
[10] T. Zhang, H. Ma, C. Zhu, J. Wang, B. Wang, Adsorption properties for heavy metal ions from aqueous solution of the novel chelating resin loaded quaternary ammonium salt, Desalin. Water Treat. (in press), doi: 10.1080/19443994.2014.927792.
[11] M. Yang, Y. Zhao, X. Sun, X. Shao, D. Li, Adsorption of Sn(II) on expanded graphite: Kinetic and equilibrium isotherm studies, Desalin. Water Treat. 52 (2014) 283–292.
[12] E.T. Wong, K.H. Chan, M. Irfan, A. Idris, E. Misran, Enhanced removal of Cu(II) by photocatalytic reduction using maghemite PVA-alginate separable beads: Kinetic and equilibrium studies, Sep. Sci. Tech. (in press), doi: 10.1080/01496395.2014.953177.
[13] N.A.M. Zain, M.S. Suhaimi, A. Idris, Development and modification of PVA-alginate as a suitable immobilization matrix, Process Biochem. 46 (2011) 2122–2129.
[14] S.R. Pouran, A.A.A. Raman, W.M.A.W. Daud, Review on the application of modified iron oxides as heterogeneous catalysts in Fenton reactions, J. Clean Prod. 64 (2014) 24–35.

[15] Z.C. Xu, Y.L. Hou, S.H. Sun, Magnetic core/shell Fe_3O_4/Au and Fe_3O_4/Au/Ag nanoparticles with tunable plasmonic properties, J. Am. Chem. Soc. 129 (2007) 8698–8699.
[16] L. Zhao, H. Yang, Magnetic Properties of Nd^{3+}-Doped $Ni_{0.7}Mn_{0.3}Fe_2O_4$ Ferrite Nanocrystal, Mater. Manuf. Processes 23 (2007) 5–9.
[17] T.M. Alslaibi, I. Abustan, M.A. Ahmad, A.A. Foul, Comparative studies on the olive stone activated carbon adsorption of Zn^{2+}, Ni^{2+}, and Cd^{2+} from synthetic wastewater, Desalin. Water Treat. (in press), doi: 10.1080/19443994.2013.876672.
[18] W. Brullot, N.K. Reddy, J. Wouters, V.K. Valev, B. Goderis, J. Vermant, T. Verbiest, Versatile ferrofluids based on polyethylene glycol coated iron oxide nanoparticles, J. Magn. Magn. Mater. 324 (2012) 1919–1925.
[19] A.S. Karakoti, S. Das, S. Thevuthasan, S. Seal, PEGylated inorganic nanoparticles, Angew. Chem. Int. Ed. 50 (2011) 1980–1994.
[20] K.H. Chan, E.T. Wong, M.I. Khan, A. Idris, N.M. Yusof, Fabrication of polyvinylidene difluoride nano-hybrid dialysis membranes using functionalized multiwall carbon nanotube for polyethylene glycol (hydrophilic additive) retention, J. Ind. Eng. Chem. 20 (2014) 3744–3753.
[21] S. Chakrabarti, S.K. Mandal, S. Chaudhuri, Cobalt doped γ-Fe2O3 nanoparticles: Synthesis and magnetic properties, Nanotechnology. 16 (2005) 506–511.
[22] Z. Aksu, I.A. İşoğlu, Removal of Copper (II) ions from aqueous solution by biosorption: Onto agricultural waste sugar beet pulp, Process Biochem. 40 (2005) 3031–3044.
[23] Y.S. Jung, M. Pyo, Removal of heavy metal ions by electrocoagulation for continuous use of Fe^{2+}/Fe^{3+}-mediated electrochemical oxidation solutions, Bull. Korean Chem. Soc. 29 (2008) 974–978.
[24] M.A. Barakat, New trends in removing heavy metals from industrial wastewater, Arabian J. Chem. 4 (2011) 361–377.
[25] G. Bossard, G. Briggs, T. Stow, Optimizing chlorination/dechlorination at a wastewater treatment plant, Public Works. 126 (1995) 33–35.
[26] United States Environmental Protection Agency Wastewater Technology Fact Sheet: Dechlorination, EPA 832-F-00-022.
[27] A. Idris, N.S.M. Ismail, N. Hassan, E. Misran, A. Ngomsik, Synthesis of magnetic alginate beads based on maghemite nanoparticles for Pb(II) removal in aqueous solution, J. Ind. Eng. Chem. 18 (2012) 1582–1589.
[28] Z. Shan, W. Yang, X. Zhang, Q. Huang, H. Ye, Preparation and characterization of carboxyl-group functionalized superparamagnetic nanoparticles and the potential for bio-applications, J. Braz. Chem. Soc. 18 (2009) 1329–1335.
[29] H. Cui, W. Ren, W. Wang, Synthesis on an ultra large scale of nearly monodispersed γ-Fe_2O_3 nanoparticles with La(III) doping through a sol–gel route assisted by propylene oxide, J. Sol–Gel Sci. Technol. 54 (2010) 37–41.
[30] A. Siciliano, M.A. Stillitano, S. De Rosa, Increase of the anaerobic biodegradability of olive mill wastewaters through a pre-treatment with hydrogen peroxide in alkaline conditions, Desalin. Water Treat. (in press), doi: 10.1080/19443994.2014.928797.
[31] C. Zhan, M. Zhong, F. Chen, J. Yang, X. Cao, X. Jiang, Decolorization of rhodamine B using hydrogen peroxide and $H_3PW_{12}O_{40}$@C photocatalyst synthesized *in situ* under ultraviolet irradiation, Desalin. Water Treat. (in press), doi: 10.1080/19443994.2013.870062.
[32] H.R. Radfarnia, M.C. Iliuta, Development of zirconium-stabilized calcium oxide absorbent for cyclic high-temperature CO_2 capture, Ind. Eng. Chem. Res. 51 (2012) 10390–10398.
[33] T.A. Kurniawan, G.Y.S. Chan, W. Lo, S. Babel, Comparisons of low-cost adsorbents for treating wastewaters laden with heavy metals, Sci. Total Environ. 366 (2006) 409–426.
[34] M.H. Dehghani, A.H. Mahvi, N. Rastkari, R. Saeedi, S. Nazmara, E. Iravani, Adsorption of bisphenol A (BPA) from aqueous solutions by carbon nanotubes: Kinetic and equilibrium studies, Desalin. Water Treat. (in press), doi: 10.1080/19443994.2013.876671.
[35] M. Kebir, M. Trari, R. Maachi, N. Nasrallah, A. Amrane, Valorization of *Inula viscosa* waste extraction, modeling of isotherm, and kinetic for the tartrazine dye adsorption, Desalin. Water Treat. (in press), doi: 10.1080/19443994.2014.905976.
[36] R.R. Krishni, K.Y. Foo, B.H. Hameed, Adsorption of cationic dye using a low-cost biowaste adsorbent: Equilibrium, kinetic, and thermodynamic study, Desalin. Water Treat. (in press), doi: 10.1080/19443994.2013.815689.
[37] A.D. Site, Factors affecting sorption of organic compounds in natural sorbent/water systems and sorption coefficients for selected pollutants. A review, J. Phys. Chem. Ref. Data 30 (2001) 187–439.
[38] Y.S. Ho, G. McKay, Application of kinetic models to the sorption of copper(II) on to peat, Adsorpt. Sci. Technol. 20 (2002) 797–815.
[39] K. Vijayaraghavan, K. Palanivelu, M. Velan, Biosorption of copper(II) and cobalt(II) from aqueous solutions by crab shell particles, Bioresour. Technol. 97 (2006) 1411–1419.
[40] Z. Aly, A. Graulet, N. Scales, T. Hanley, Removal of aluminium from aqueous solutions using PAN-based adsorbents: Characterisation, kinetics, equilibrium and thermodynamic studies, Environ. Sci. Pollut. Res. Int. 21 (2014) 3972–3986.
[41] Z. Aly, V. Luca, Uranium extraction from aqueous solution using dried and pyrolyzed tea and coffee wastes, J. Radioanal. Nucl. Chem. 295 (2013) 889–900.